SUPPLEMENTARY MATERIALS D. A. RUCHKIN, ET AL. "THE TWO KEY SUBSTITUTIONS IN THE CHROMOPHORE ENVIRONMENT OF mKate2 TO PRODUCE AN ENHANCED FUSIONRED-LIKE RED FLUORESCENT PROTEIN"

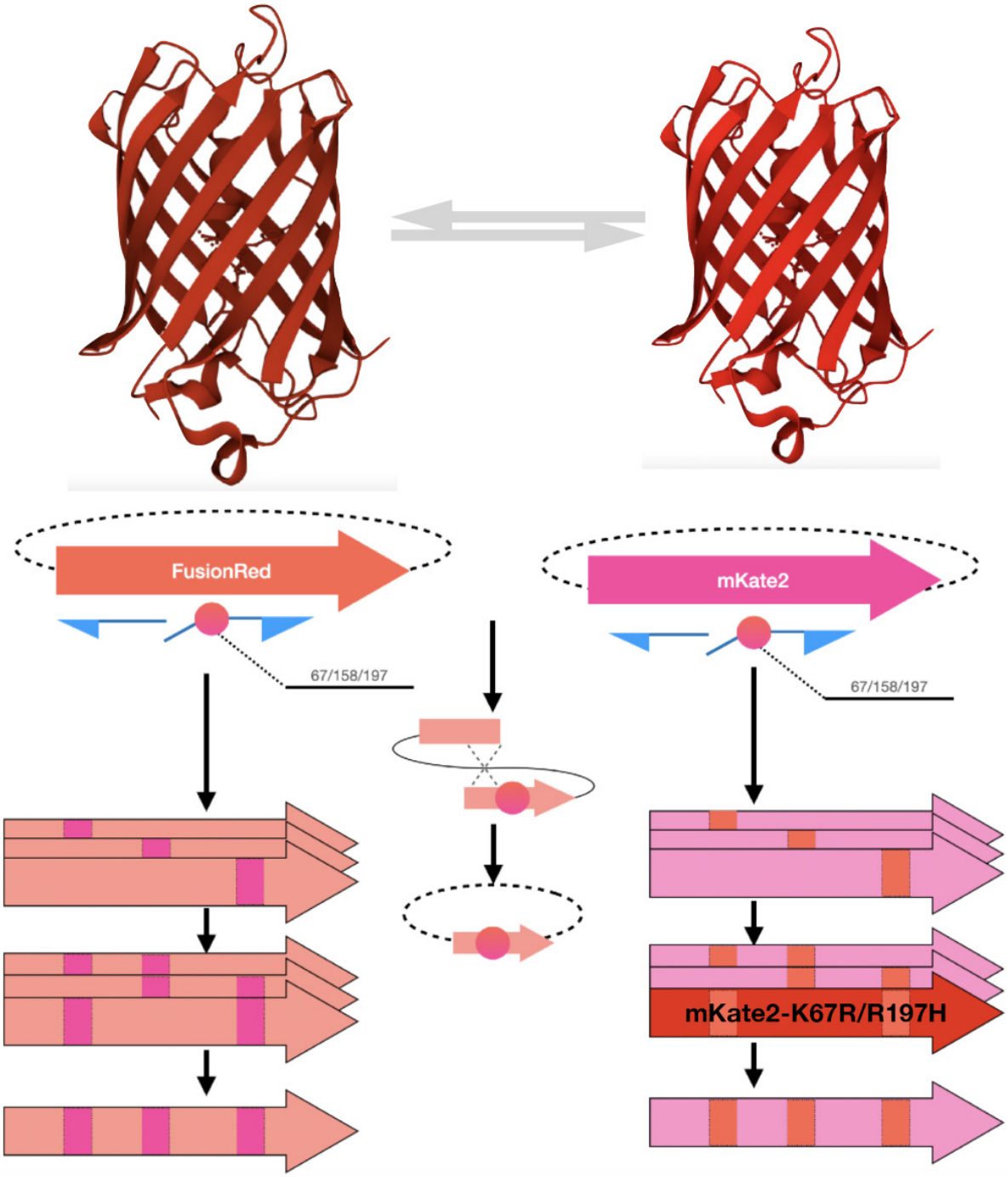

Fig. S1. Scheme showing how the library of point reciprocal mutants used in this study was engineered. The upper panel illustrates a general idea of 'exchanging' amino acid residues at positions 67/158/197 between the original FusionRed and mKate2 proteins. In the center of the scheme, there is a principle of IVA-cloning-based site-directed mutagenesis explained graphically (blue arrows are oligonucleotides; pink circles are DNA mismatches with substituted codons; dashed-lined ellipses depict vector backbone; the dotted cross shows recombination and ligation of the full-vector-PCR product). Aligned thick arrows on the left and right represent particular variants carrying single, double, and triple (single arrow) substitutions (mutated sites are shown as vertical bands of the "opposite" color)

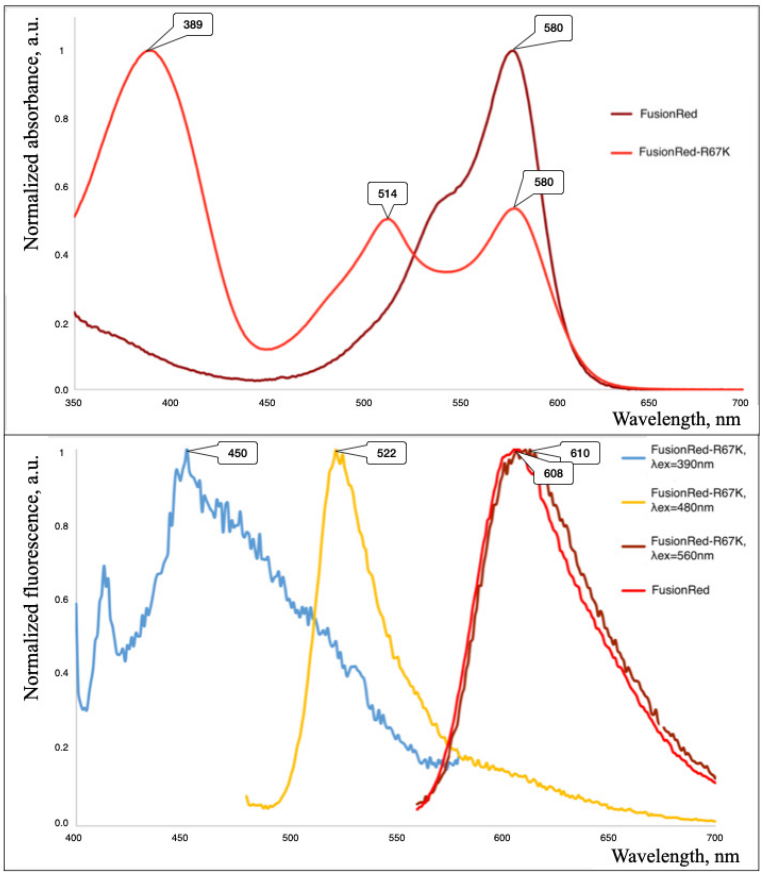

Fig. S2. Absorption (*A*) and fluorescence emission (*B*) spectra of FusionRed-R67K compared with those of its parent FusionRed. Wavelengths of the maxima of major bands are shown in the bubbles. In the fluorescence graph, excitation wavelengths used for recording the emission spectra are shown in the legend (the right upper corner)

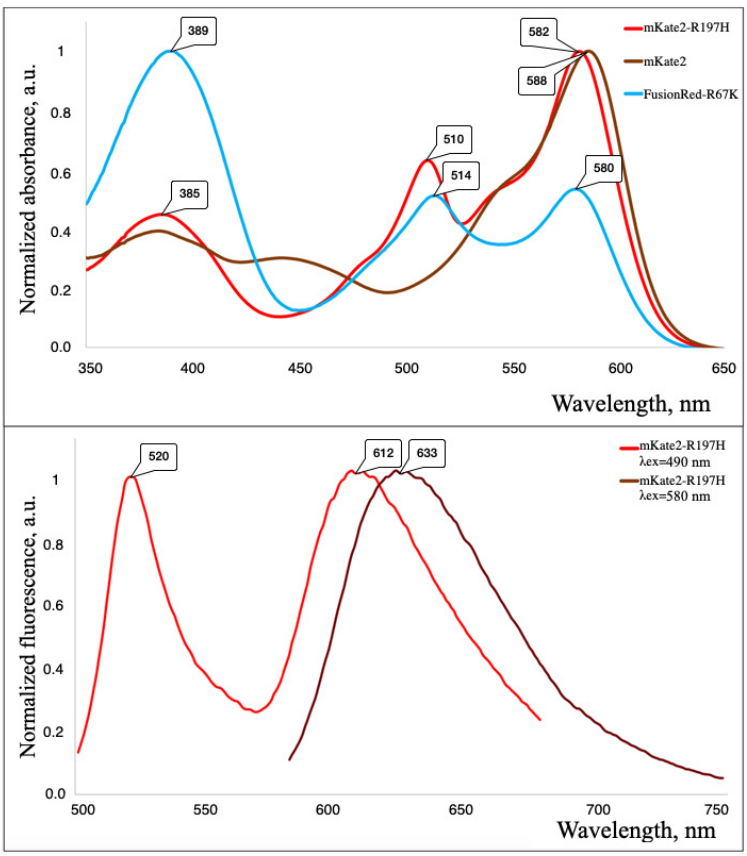

Fig. S3. Absorption (*A*) and fluorescence emission (*B*) spectra of mKate2-R197H compared with those of its parent mKate2. Wavelengths of the maxima of major bands are shown in the bubbles. In the absorption graph, the spectrum of FusionRed-R67K (solid blue line) is also added as a reference. In the fluorescence graph, excitation wavelengths used for recording the emission spectra are shown in the legend (the right upper corner)

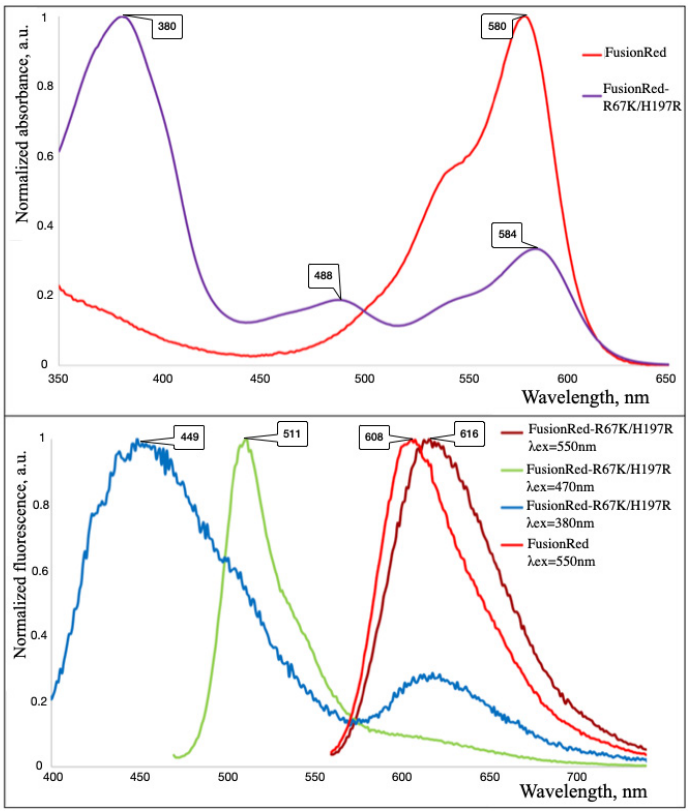

Fig. S4. Absorption (*A*) and fluorescence emission (*B*) spectra of FusionRed-R67K/H197R compared with those of its parent FusionRed. Wavelengths of the maxima of major bands are shown in the bubbles. In the fluorescence graph, excitation wavelengths used for the emission spectra recording are shown in the legend (the right upper corner)

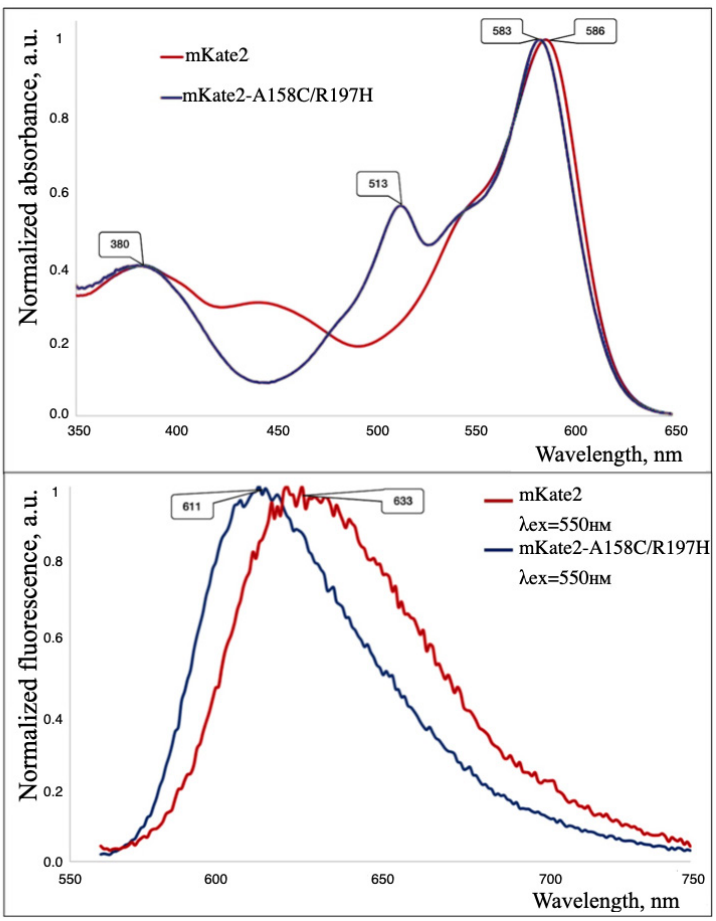

Fig. S5. Absorption (*A*) and fluorescence emission (*B*) spectra of mKate2-A158C/R197H compared with those of its parent mKate2. Wavelengths of the maxima of major bands are shown in the bubbles. In the fluorescence graph, excitation wavelengths used for recording the emission spectra are shown in the legend (the right upper corner)

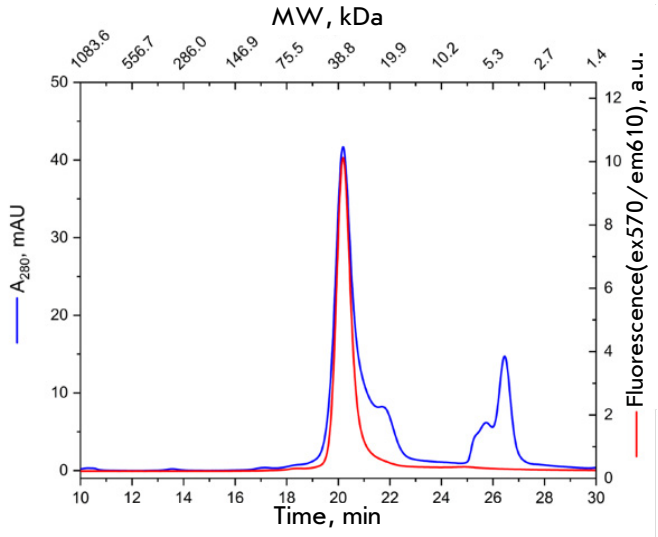

Fig. S6. Gel filtration chromatography of a purified mKate2-K67R/R197H (Diogenes) sample. Eluate was monitored using in-line absorbance and fluorescence detectors.

Table S1. Protein standards used to calibrate a gel filtration setup. The leftmost column represents the protein name; the central, molecular weight, kDa; the rightmost one, elution time while calibrating

Protein	Molecular mass, kDa	Elution time, min
CytochromeC, horse heart	12.4	23.354
Carboanhydrase, bovine erythrocytes	29	21.265
BSA	66	17.767
Alcohol dehydrogenase, yeast	150	15.995
β-amylase, sweet potato	200	15.253
Ferritin, horse spleen	450	12.723

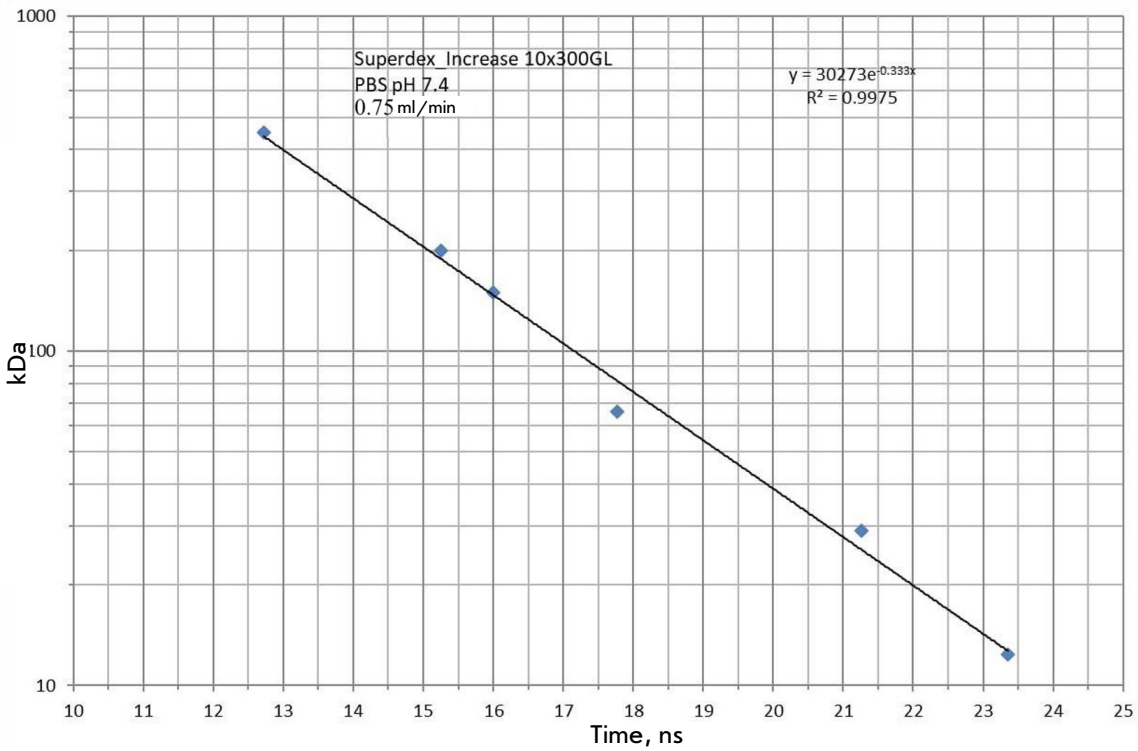

Fig. S7. Calibration plot used to determine molecular weights in the gel filtration/liquid chromatography setup (see the Materials and Methods section, main text). Blue squares show the protein standards used for calibration. Column type and equilibration/elution parameters, as well as the linear fitting results, are described on the graph

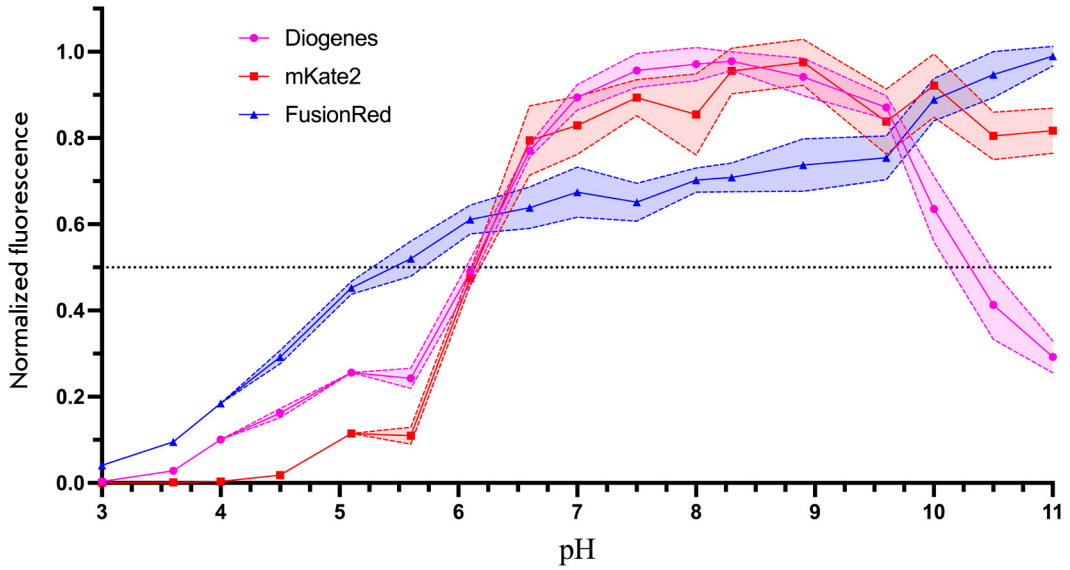

Fig. S8. Graph showing the fluorescence intensity dependence on pH (pH stability) measured for the purified mKate2-K67R/R197H (Diogenes), mKate2 and FusionRed proteins. The signal at each measurement point was normalized to a maximum signal value within the dataset

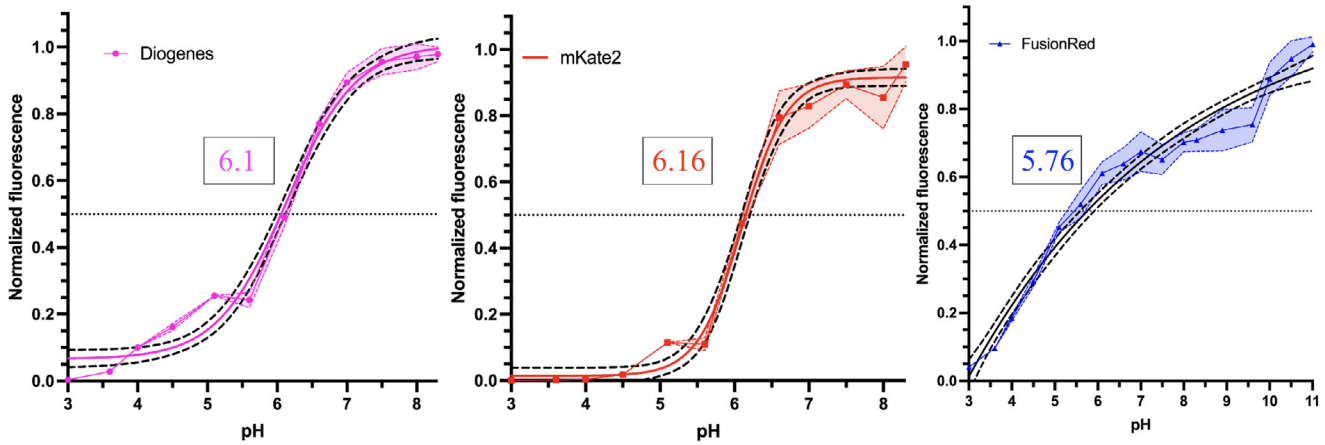

Fig. S9. Sigmoidal fits of the pH stability data for Diogenes, mKate2, and FusionRed. Colored graphs represent experimental data with standard deviations shown as semi-transparent areas ($n = 6$). The solid black line is the fitting curve with 95% confidence bands shown in black dashed lines. Fitting was performed using the GraphPad Prism10 package (the four-parameter logistic curve (4PL) fitting mode was used). The horizontal line stands for the half-maximum fluorescence level

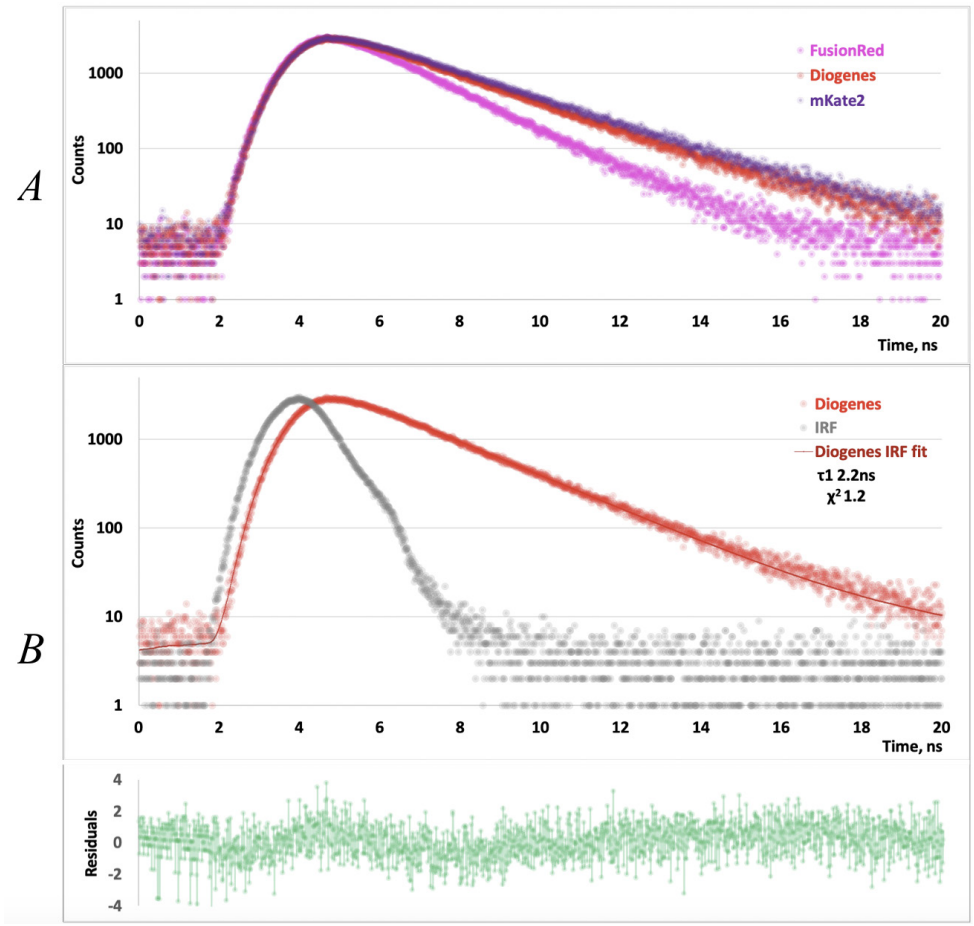

Fig. S10. The fluorescence decay kinetics recorded upon 590 nm single-photon excitation with the nanosecond pulsed LED driven at a repetition rate of 20 MHz. Comparison of the raw-data decay curves for FusionRed, mKate2, and Diogenes (*A*). Single-component exponential fitting of the Diogenes decay curve (*B*). Deconvolution with IRF was used for fitting. The measured instrument response (IRF) is shown in red

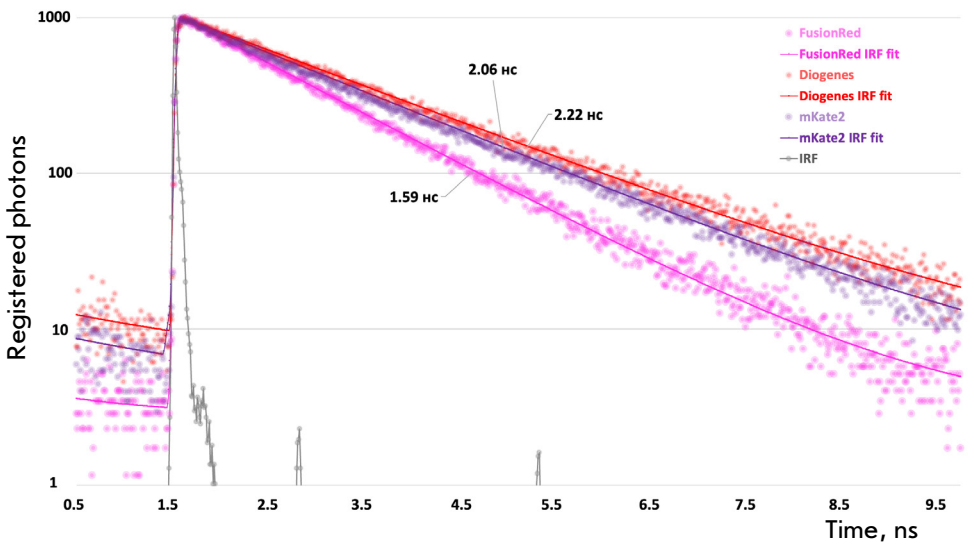

Fig. S11. The fluorescence decay kinetics recorded upon 590 nm single-photon excitation with the femtosecond laser driven at a repetition rate of 80 MHz. The raw-data and exponential fitting curves for FusionRed (biexponential fit), mKate2 and Diogenes (monoexponential fits) are shown. Mean lifetime values are inscribed next to the decay curves. Deconvolution with IRF was used for fitting. The measured instrument response (IRF) is shown in gray

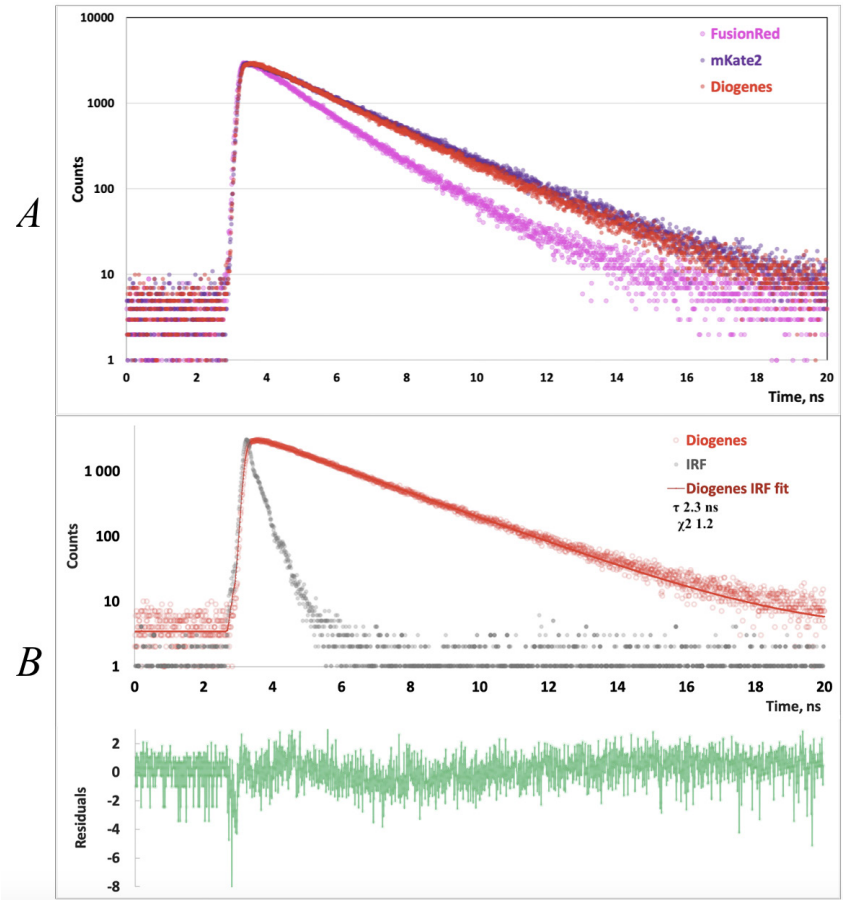

Fig. S12. The fluorescence decay kinetics recorded upon 450 nm single-photon excitation with the picosecond diode laser driven at a repetition rate of 20 MHz. Comparison of the raw-data decay curves for FusionRed, mKate2 and Diogenes (*A*). Single-component exponential fitting of the Diogenes decay curve (*B*). Deconvolution with IRF was used for fitting. The measured instrument response (IRF) is shown in gray

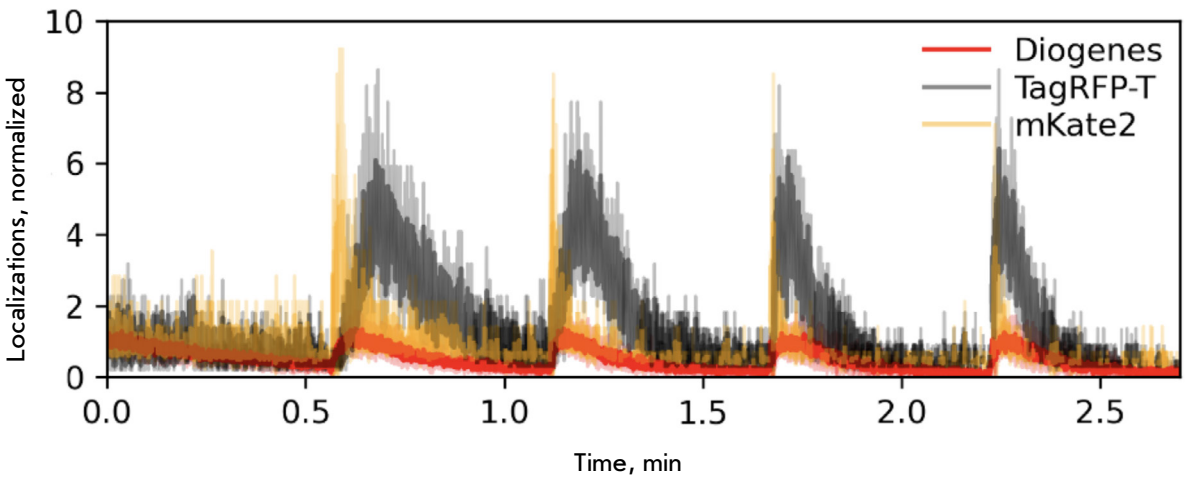

Fig. S13. The effect of 405 nm laser illumination on the localization density of Diogenes, TagRFP-T, and mKate2 as parts of vimentin fusion proteins in live HeLa cells during imaging under the following conditions: 2 kW/cm^2 561 nm laser, 16.7 ms frame time, 10,000 frames. Laser pulses were applied every 22 s with a duration of 405 nm laser illumination of 0.4 s and illumination density of ~215 W/cm^2